Evaporation of Seawater: Calculated Mineral Sequences

Abstract. *Van't Hoff's predictions of the mineral sequences to be expected on the evaporation of seawater are based on an oversimplified system. New computer calculations that include calcium-bearing phases are in better agreement with natural occurrences, removing discrepancies that have plagued evaporite geologists for nearly a century. A new hydrologic model that combines equilibrium batch evaporation with fractionation between successive batches is proposed to account for the mineral sequences observed in such classic deposits as the German Zechstein.*

Between 1896 and 1908, Van't Hoff and his co-workers carried out a massive experimental program designed to elucidate marine evaporite deposits. Their results correlated surprisingly well with mineral sequences observed in the Permian Zechstein of Germany (*1*). Nevertheless, Van't Hoff was keenly aware of major discrepancies between prediction and observation. He concluded [as quoted in (*2*), p. 486] that

> These results correlate with natural relationships qualitatively, but not at all quantitatively, which indicates that salt deposits are not formed by simple evaporation of seawater.

The three most important discrepancies are related to (i) the ratio of anhydrite to halite, which is much higher in natural deposits than predicted; (ii) the absence of kainite; and (iii) the presence of sylvite, which appears in the predicted sequences only at temperatures above 83°C. Subsequent workers have invoked metastable crystallization, metamorphism, and temperature or concentration gradients to account for the discrepancies. None of these explanations has proved fully satisfactory. The validity of the mineral sequences predicted by Van't Hoff and his co-workers from solubility experiments in the simplified, calcium-free system has never been challenged. We present here a new predicted mineral sequence based on solubility calculations in the system Ca-Na-K-Mg-Cl-SO_4-H_2O. This sequence is in better accord with natural occurrences.

The ideal mineral sequence predicted by Van't Hoff and subsequent workers is based on mineral equilibria in the calcium-free seawater system Na-K-Mg-Cl-SO_4-H_2O at halite saturation, customarily depicted in a Jänecke projection [(*3*), p. 84; (*4*), p. 12; (*5*)]. Because Ca^{2+} and HCO_3^- are not included in these equilibria, the composition of seawater is adjusted by removing all HCO_3^- as calcite and the remaining Ca^{2+} is combined with SO_4^{2-} in gypsum. This procedure was thought to be permissible because little calcium is present in the late-stage saturated brines. However, except for fractional crystallization, this assumption is untenable because of possible back-reaction of the solution with early-formed anhydrite or gypsum to produce polyhalite [$K_2MgCa_2(SO_4)_4 \cdot 2H_2O$] or glauberite [$Na_2Ca(SO_4)_2$].

Progress in the phenomenological description of brine thermodynamics by Pitzer (*6*) and calculated mineral solubilities by Harvie and Weare (*7*) have made it possible to accurately predict the appropriate equilibria for carbonate-free seawater composition, at 25°C, including the crucial calcium sulfate minerals. Figure 1b shows the mineral sequences and masses to be expected on the evaporation of seawater at 25°C if it is assumed that solids are in equilibrium with the solution at all times. The resulting path has been projected onto the calcium-free system in Fig. 1a. It differs significantly from earlier predictions in that glauberite is a stable phase, whereas bloedite [$Na_2Mg(SO_4)_2 \cdot 4H_2O$] and kainite ($KMgClSO_4 \cdot 11/4H_2O$) do not appear (*3*-*5*). The new and old predictions are compared in Table 1. Our calculations indicate that glauberite should appear after halite by reaction of anhydrite ($CaSO_4$) with the brine:

$$CaSO_4 + 2Na^+ + SO_4^{2-} \rightarrow Na_2Ca(SO_4)_2$$

Eventually, glauberite is replaced in part by anhydrite and then both are replaced by polyhalite:

$$Na_2Ca(SO_4)_2 + CaSO_4 + 2K^+ + Mg^{2+} + SO_4^{2-} + 2H_2O \rightarrow K_2MgCa_2(SO_4)_4 \cdot 2H_2O + 2Na^+$$

After glauberite is consumed, polyhalite continues to form at the expense of anhydrite

$$2CaSO_4 + 2K^+ + Mg^{2+} + 2SO_4^{2-} + 2H_2O \rightarrow K_2MgCa_2(SO_4)_4 \cdot 2H_2O$$

and coprecipitates with the magnesium sulfates epsomite ($MgSO_4 \cdot 7H_2O$), hexahydrite ($MgSO_4 \cdot 6H_2O$), and kieserite ($MgSO_4 \cdot H_2O$). When carnallite ($KMgCl_3 \cdot 6H_2O$) joins the assemblage, the solution composition remains invariant until polyhalite is consumed by the reaction

$$K_2MgCa_2(SO_4)_4 \cdot 2H_2O + Mg^{2+} + 6Cl^- + 10H_2O \rightarrow 2KMgCl_3 \cdot 6H_2O + 2CaSO_4 + 2SO_4^{2-}$$

Eventually, bischofite ($MgCl_2 \cdot 6H_2O$) forms as part of the final invariant assemblage halite + kieserite + carnallite + anhydrite + bischofite + solution. The profound influence of polyhalite on the evaporation path is shown in Fig. 1a. Once polyhalite forms, the path moves away from the K_2 apex and thus skirts the kainite field. After epsomite forms, the path follows the polyhalite-anhydrite boundary to the carnallite field.

In contrast, the fractionation path, in which it is assumed that any phase which crystallizes is immediately removed from interaction with the solution, produces a different mineral sequence and different mineral masses (see Fig. 1a). In addition to the minerals found during equilibrium evaporation, we now also encounter bloedite and kainite, which appear between polyhalite and carnallite. In order of appearance, this mineral sequence is the same as that predicted for equilibrium in the past (Table 1). This is not surprising, since those predictions did not allow the earlier-formed $CaSO_4$ minerals to back-react with the solution.

The significance of the new evaporation paths can only be tested in the geologic record. If equilibrium conditions were important, we should have evidence that glauberite formed prior to the appearance of polyhalite, and that bloedite and kainite are absent. The observed assemblages in two of the best-known potash deposits of the world, the Permian Zechstein II of Germany and the Permian Salado of Texas and New Mexico, compare favorably with the equilibrium sequence (Table 1), which accounts not only for the presence of glauberite and the absence of kainite but also for the pseudomorphous replacement of gypsum and anhydrite by glauberite and polyhalite and the replacement of glauberite by polyhalite [(*3*), pp. 157 and 161; (*4*), p. 41; (*8*)]. In the past, these features have been attributed to solution and thermal metamorphism (*3*-*5*). Figure 1c compares the mineral sequence in the Zechstein II profile with the predicted equilibrium sequence for similar stages of evaporation. Except for the uppermost carnallite zone of Zechstein II, the agreement is excellent with respect to the order of appearance of minerals and their mass ratios. No quantitative field data are available for glauberite. Polyhalite and anhydrite are inversely related, and the polyhalite disappearance coincides with the formation of carnallite. The final stages of Zechstein II, where carnallite and kieserite are dominant, cannot be due to simple evaporation; this stage may be characterized by fractional dissolution and reprecipitation

0036-8075/80/0502-0498$00.50/0 Copyright © 1980 AAAS

Table 1. Comparison of the Zechstein II sequence with that predicted for modern seawater evaporation at 25°C. Abbreviations: G, gypsum; A, anhydrite; H, halite; Gl, glauberite; Po, polyhalite; Bl, bloedite; Ep, epsomite; Hx, hexahydrite; Ki, kieserite; Ka, kainite; Car, carnallite; and Bi, bischofite.

Equilibrium bitterns calcium-free (*3-5*)	Fractionation, with calcium (*14*)	Equilibrium, with calcium (*14*)	Observed, Zechstein II (*12*)
G	G	G	
A	A	A	A
A + H	A + H	A + H	A + H
	Gl + H	Gl + A + H	Gl + A + H
Po + H	Po + H	Po + A + H	Po + A + H
Bl + H	Bl + Po + H		
Ep + H	Ep + Po + H	Ep + Po + A + H	
Ka + Ep + H	Ka + Ep + Po + H		
Ka + Hx + H	Ka + Po + H	Hx + Po + A + H	
	Ka + H		
Ka + Ki + H	Ka + Ki + H	Ki + Po + A + H	Ki + Po + A + H
Car + Ki + H	Car + Ki + H	Car + Ki + Po + A + H	Car + Ki + Po + A + H
		Car + Ki + A + H	Car + Ki + A + H
Bi + Car + Ki + H	Bi + Car + Ki + H	Bi + Car + Ki + A + H	

processes typical of ephemeral salt pans (*9*).

Zechstein II could not have formed by a one-stage equilibrium evaporation of seawater, because it would require at least 8 km of seawater to produce the halite layer alone and earlier-formed phases such as polyhalite and glauberite would not be preserved. In fact, the observation that the equilibrium mineral sequence is preserved in the Zechstein II places strong constraints on the depositional process that must have occurred. In order to reconcile the apparent contradictions between equilibrium processes, preservation of a progressive sequence consisting of early reaction phases, and the observed nonequilibrium thickness relationships, we propose a new hydrologic model (*10*). Evaporation is assumed to proceed in a stratified brine basin as an equilibrium batch process. Each batch of fresh seawater added evaporates until its density is the same as that of the underlying brine. Minerals precipitated settle through the lower brine, but only those in equilibrium with that brine can accumulate at the bottom. Hence the minerals that are deposited are defined by the concentration stage of the lower brine. When the upper brine reaches the same stage, that is, when the pycnocline disappears, the two brines mix. Continued evaporation of the mixed brine raises its density and produces the appropriate mineral sequence. The next batch of fresh seawater added must evaporate further than the previous batch before it can mix. The increment of precipitates it contributes covers the earlier precipitates and protects them from fully back-reacting with the open brine, thus preserving glauberite and polyhalite. We believe that successive batches progressively evaporated in this manner will produce the mineral sequence observed in Zechstein II.

The assumption of a single brine body

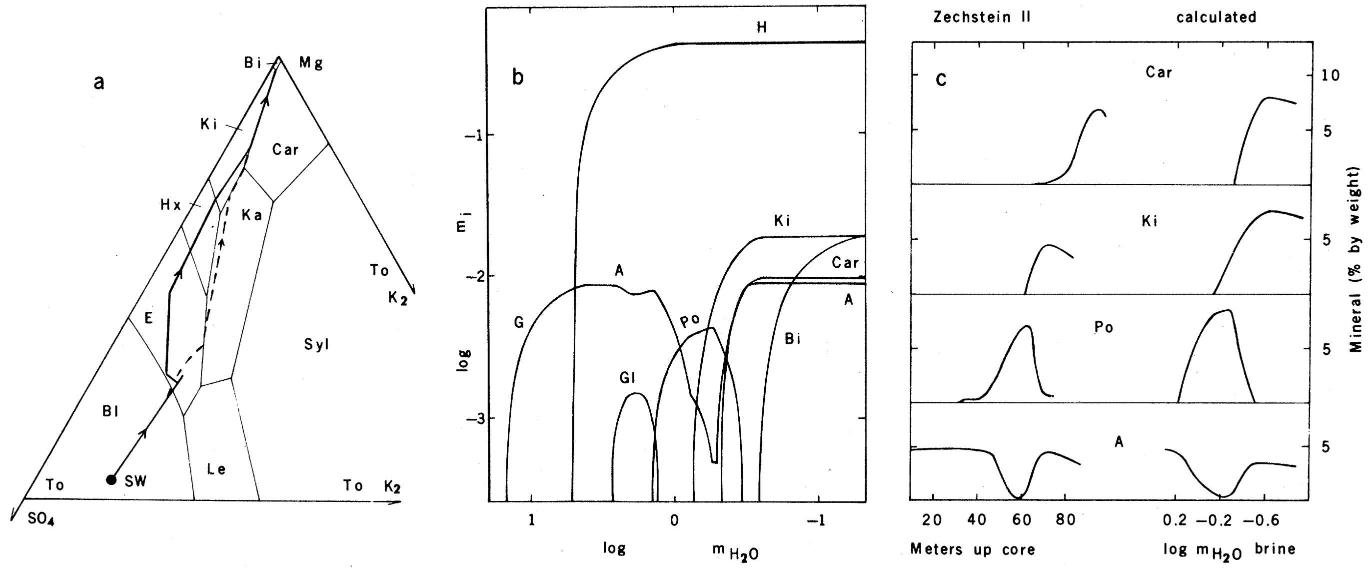

Fig. 1. Seawater (*SW*) evaporation path, mineral precipitation, and comparison with mineral abundances in Zechstein II (Stassfurt). (a) A portion of the Jänecke projection for K_2-Mg-SO_4 at halite saturation, as calculated by Harvie and Weare (*7*). The solid line is the evaporation path for seawater in the calcium-bearing system under equilibrium conditions at 25°C. The dashed line is for evaporation under conditions of fractional crystallization. Abbreviations: *Bl*, bloedite; *Le*, leonite; *E*, epsomite; *Hx*, hexahydrite; *Ki*, kieserite; *Syl*, sylvite; *Ka*, kainite; *Car*, carnallite; *Bi*, bischofite. (b) The predicted precipitation of minerals during seawater evaporation; m_{H_2O} is the number of moles of water remaining in the brine, and evaporation starts on the left with 55.5 moles of water. Both epsomite and hexahydrite are included in kieserite. Abbreviations: *G*, gypsum; *A*, anhydrite; *H*, halite; *Gl*, glauberite; *Po*, polyhalite. (c) Comparison of mineral abundances (with halite making up the remainder) in Zechstein II, after Riedel (*12*), as a function of depth in the core (bottom left), with amounts expected to precipitate by calculation [from (b)]. Comparable stages of evaporation are indicated by depth (left) and m_{H_2O} (right).

which increases in concentration progressively is supported by the bromine profile of the Zechstein II. The bromine:chlorine ratio of halite increases smoothly upward in the section, in marked contrast to its erratic behavior reported from other deposits (*11*).

The new predicted evaporation path for seawater has removed mineralogical discrepancies with observed sequences including glauberite, polyhalite, and kainite. We offer no insight into the presence of sylvite, which often is considered to be secondary after carnallite (*12*, *13*). The new hydrologic model can account for the observed anhydrite-halite mass relationships without the need to assume reflux or sulfate enrichment. By comparing the mineral sequences observed in a particular evaporite deposit with the predictions obtained in the more complete system, it may be possible to evaluate the contributions of stable equilibrium, metastable equilibrium, and fractional crystallization processes.

CHARLES E. HARVIE, JOHN H. WEARE
Department of Chemistry,
University of California, San Diego,
La Jolla 92093

LAWRENCE A. HARDIE
HANS P. EUGSTER
Department of Earth and Planetary
Sciences, Johns Hopkins University,
Baltimore, Maryland 21218

References and Notes

1. J. H. Van't Hoff, *Zur Bildung der ozeanischen Salzlagerstätten* [Vieweg, Braunschweig, 1905 (first part) and 1909 (second part)].
2. H. P. Eugster, *Science* **173**, 481 (1971).
3. O. Braitsch, *Salt Deposits: Their Origin and Composition* (Springer-Verlag, New York, 1971).
4. F. H. Stewart, *U.S. Geol. Surv. Prof. Pap. 440-Y* (1963).
5. H. Borchert and R. O. Muir, *Salt Deposits* (Van Nostrand, London, 1964), pp. 64-76; W. T. Holser, *Mineralogy of Evaporites* (Short Course Notes 6, Mineralogical Society of America, Washington, D.C., 1979), pp. 211-294.
6. K. S. Pitzer, *J. Phys. Chem.* **77**, 268 (1973).
7. C. E. Harvie and J. H. Weare, *Geochim. Cosmochim. Acta*, in press.
8. W. T. Schaller and E. P. Henderson, *U.S. Geol. Surv. Bull. 833* (1932).
9. H. P. Eugster and L. A. Hardie, *Geol. Soc. Am. Bull.* **86**, 319 (1975); in *Lakes: Chemistry, Geology, Physics*, A. Lerman, Ed. (Springer-Verlag, New York, 1978), pp. 237-293; L. A. Hardie, *Geochim. Cosmochim. Acta* **32**, 1279 (1968); M. G. Valyashko, *Geology of Saline Deposits* (Proceedings of the Hanover Symposium, Unesco, New York, 1972), pp. 41-51.
10. L. A. Hardie *et al.*, in *Modern and Ancient Lake Sediments*, A. Matter and M. E. Tucker, Eds. (Special Publication 2, International Association of Sedimentologists, Blackwell, London, 1978); compare with R. F. Schmalz, *Am. Assoc. Pet. Geol. Bull.* **53**, 798 (1969).
11. W. T. Holser, *Second Symp. Salt No. Ohio Geol. Soc.* **2**, 248 (1966), figure 8; R. Kühn, *Geol. Soc. Am. Spec. Pap. 88* (1968), figure 3B.
12. O. Riedel, *Z. Kristallogr.* **50**, 139 (1912).
13. N. C. Wardlaw, *Geol. Soc. Am. Bull.* **79**, 1273 (1968).
14. C. E. Harvie, J. H. Weare, L. A. Hardie, H. P. Eugster, *Geol. Soc. Am. Abstr. Programs* **11**, 440 (1979).
15. Work supported by NSF grants 7810491 and EAR 7903875.

14 December 1979; revised 7 February 1980

Selenium Biomethylation Products from Soil and Sewage Sludge

Abstract. *Inorganic selenium compounds are converted to volatile methylated species (dimethyl selenide, dimethyl diselenide, and dimethyl selenone or methyl methylselenite) by microorganisms in sewage sludge and soil. In the absence of added selenium, no volatile selenium compounds were detected. All samples were evaluated without the addition of nutrients and in the presence of air or nitrogen. The methylation process may be an important step in the detoxification process for microorganisms exposed to high concentrations of selenium.*

In trace amounts selenium is essential for human health, but at higher concentrations it can be harmful (*1*). Concentrations of atmospheric selenium in remote areas of the earth are far in excess of predictions from anthropogenic or known natural sources (*2*). Up to 50 percent of the atmospheric selenium passes through filters capable of collecting 99 percent of the particles with diameters in excess of 0.1 μm (*3*). This vapor-phase, or very fine particle selenium, could be inorganic forms such as Se or SeO_2, which have relatively high vapor pressures, or organic selenium.

A potentially important source of atmospheric selenium is natural biomethylation. Selenium is known to be biomethylated, producing organic metabolites that are more volatile than the original inorganic forms (*4*). Other metals such as lead (*5*), arsenic (*6*), tin (*7*), and mercury (*8*) can also be biomethylated, forming organic compounds that are usually more toxic than the inorganic forms. Selenium is of interest as a potential environmental toxicant because of the small margin between the necessary nutritional levels and human toxicity (*9*).

Rats, plants, fungi, bacteria, molds, and microorganisms can produce methylated forms of selenium when exposed to inorganic or certain organic forms. Rats fed selenate or selenite exhale dimethyl selenide, $(CH_3)_2Se$ (*10*). Nonaccumulator plants, such as cabbage, give off $(CH_3)_2Se$, and accumulator species, such as *Astragalus racemosus*, produce dimethyl diselenide, $(CH_3)_2Se_2$, when exposed to selenite (*11*). Eleven microorganisms have been isolated from the soil that are capable of producing $(CH_3)_2Se$ (*12*). A strain of *Penicillium* that produced $(CH_3)_2Se$ from inorganic selenium compounds was isolated from raw sewage (*13*), and in the presence of air soils containing added inorganic selenium and glucose evolve $(CH_3)_2Se$ (*14*). Recently, $(CH_3)_2Se$ and an unknown volatile selenium compound were detected in an aqueous extract of biologically active lake sediment with and without added inorganic or organic selenium compounds (*6*). Since selenium is highly susceptible to biomethylation, this reaction may be an important step in its transformation and ultimate transport in the environment.

Our investigation was carried out to ascertain the quantity and the volatile forms of selenium that could be released to the atmosphere from soil and sewage sludge by methylation when selenium in different oxidation states is added under aerobic and anaerobic conditions. Soil and sewage sludge media were chosen because their high biological activities render them a likely ecosystem for biomethylation.

The selenium reactor system consisted of a 500-ml flask fitted with a ground-glass stopper containing an inlet glass tube that extended to near the bottom of the flask and an outlet tube. The inlet tube was connected to a gas cylinder and the outlet to a Teflon tube (6 cm by 1 cm in outside diameter) containing 0.25 g of Spherocarb (60 to 80 mesh) used for the room temperature collection of the gaseous selenium metabolites. A stream of either high-purity nitrogen or air was passed through the sampling flask, which contained 100 g of sewage sludge or soil, to sweep the volatile metabolites present in the headspace into the Spherocarb trap. The Spherocarb quantitatively retains organic selenium forms so that they can be extracted for subsequent chemical analysis. The flow rate was 50 to 100 ml/min, sufficient to flush the system in 10 minutes. The sewage sludge or soil was first passed through a Nuclepore filter with 0.2-μm pores to ensure the removal of any particles released from the media by physical processes. In preliminary experiments with radioactive tracer, we found that less than 5 percent of the $(CH_3)_2Se$ was retained by the Nuclepore filters and the other parts of the sampling system. The Spherocarb was treated with 3 ml of methanol, which extracts the volatile selenium metabolites quantitatively. These metabolites were analyzed with a gas chromatograph–microwave plasma detector system which is specific for the identification of selenium compounds and is capable of detecting as little as 20 pg of $(CH_3)_2Se$ (*15*).

We confirmed $(CH_3)_2Se$ and $(CH_3)_2Se_2$ by gas chromatography-mass spectrom-